NeuroImage 88 (2014) 252–262

Contents lists available at ScienceDirect

NeuroImage

journal homepage: www.elsevier.com/locate/ynimg

Regional differences in SERT occupancy after acute and prolonged SSRI intake investigated by brain PET

Pia Baldinger [a,1], Georg S. Kranz [a,1], Daniela Haeusler [b], Markus Savli [a], Marie Spies [a], Cecile Philippe [b], Andreas Hahn [a], Anna Höflich [a], Wolfgang Wadsak [b], Markus Mitterhauser [b], Rupert Lanzenberger [a,*], Siegfried Kasper [a]

[a] Department of Psychiatry and Psychotherapy, Medical University of Vienna, Austria
[b] Department of Biomedical Imaging and Image-guided Therapy, Division of Nuclear Medicine, Medical University of Vienna, Austria

ARTICLE INFO

Article history:
Accepted 1 October 2013
Available online 11 October 2013

Keywords:
Antidepressant
Occupancy
PET
Serotonin transporter
Subgenual cingulate cortex

ABSTRACT

Blocking of the serotonin transporter (SERT) represents the initial mechanism of action of selective serotonin reuptake inhibitors (SSRIs) which can be visualized due to the technical proceedings of SERT occupancy studies. When compared to the striatum, higher SERT occupancy in the midbrain and lower values in the thalamus were reported. This indicates that occupancy might be differently distributed throughout the brain, which is supported by preclinical findings indicating a regionally varying SERT activity and antidepressant drug concentration. The present study therefore aimed to investigate regional SERT occupancies with positron emission tomography and the radioligand [^{11}C]DASB in 19 depressed patients after acute and prolonged intake of oral doses of either 10 mg/day escitalopram or 20 mg/day citalopram. Compared to the mean occupancy across cortical and subcortical regions, we detected increased SERT occupancies in regions commonly associated with antidepressant response, such as the subgenual cingulate, amygdala and raphe nuclei. When acute and prolonged drug intake was compared, SERT occupancies increased in subcortical areas that are known to be rich in SERT. Moreover, SERT occupancy in subcortical brain areas after prolonged intake of antidepressants was predicted by plasma drug levels. Similarly, baseline SERT binding potential seems to impact SERT occupancy, as regions rich in SERT showed greater binding reduction as well as higher residual binding. These findings suggest a region-specific distribution of SERT blockage by SSRIs and relate the postulated link between treatment response and SERT occupancy to certain brain regions such as the subgenual cingulate cortex.

Introduction

In the last decades, molecular imaging studies applying positron emission tomography (PET) have yielded new insights into antidepressant drug action, the neurobiological correlates of clinical response and the superiority of certain agents (Kasper et al., 2009; Talbot and Laruelle, 2002). For example, Meyer et al. investigated serotonin transporter (SERT) occupancy in 77 subjects after a month long intake of five different SSRIs. The authors consistently showed occupancy levels of approximately 80% in the striatum across all antidepressants applied at minimum therapeutic doses and suggested that this value might be a necessary minimum for adequate treatment (Meyer et al., 2004). Interestingly, in addition to striatal SERT binding, this study also focused on occupancy levels in other brain regions, revealing a higher SERT occupancy in the midbrain (8% higher) and lower values in the thalamus (8% lower) when compared to the striatum. This indicates that SERT occupancy might not be equally distributed throughout the brain. Furthermore, it is well known from PET studies that SERT binding and availability is differently distributed within the brain, ranked in the order e.g.: midbrain > thalamus > striatum > cingulate > other cortical regions > cerebellum (Kranz et al., 2010; Savli et al., 2012) and one may consider a dependence of occupancy values on SERT availability. However, investigations into the regional distribution of SERT occupancy remain scarce.

Three conceivable scenarios describe the relationship between SERT occupancies and SERT density: In scenario 1, SERT occupancy is equally distributed across brain regions. Occupancy is defined as percent signal reduction (1 − SERT availability at treatment/SERT availability at baseline) × 100; thus, absolutely more SERTs are blocked in regions with higher SERT density. Scenario 1 becomes plausible when considering the basic principles of a chemical reaction. According

* Corresponding author at: Functional, Molecular & Translational Neuroimaging Lab, Department of Psychiatry and Psychotherapy, Medical University of Vienna, Waehringer Guertel 18-20, 1090 Vienna, Austria.
E-mail address: rupert.lanzenberger@meduniwien.ac.at (R. Lanzenberger).
[1] Contributed equally.

1053-8119/$ – see front matter © 2013 Elsevier Inc. All rights reserved.
http://dx.doi.org/10.1016/j.neuroimage.2013.10.002

to the law of mass action, the amount of bound SERTs should be proportional to the product of free drug concentration, SERT availability and affinity, given by the equation

$$\frac{B}{B_{max}} = F * \frac{B_{avail}}{B_{max}} * \frac{1}{K_D} \quad (1)$$

where B/B_{max} equals SERT occupancy, F indicates the free drug concentration, B_{avail}/B_{max} the available SERTs relative to SERT density and $1/K_D$ equals the affinity. Deviations from Scenario 1 may occur when drug concentrations and dissociation constants (i.e., concentration of free drug at which 50% of total SERT is blocked by the drug) are heterogeneously distributed across brain regions. Therefore, we define scenarios 2 and 3 as states, where less or more SERTs are occupied in regions with higher SERT density, respectively.

Several lines of evidence hint towards the possibility of non-homogenous SERT occupancy and relate it to drug plasma levels, thus challenging scenario 1. Kugelberg et al. showed that citalopram concentrations differ between brain regions in a series of animal studies (Kugelberg et al., 2001, 2003). Concentrations were twofold higher in the cortex than in the midbrain of rats. These differences in concentration were suggested to depend on regional differences in blood flow and lipophilicity. Affinity of citalopram, on the other hand, seems to be a constant variable throughout brain regions, namely the brainstrem, the basal ganglia and the frontal cortex (Zeng et al., 2006). However, lipophilicity does seem to partly determine tracer affinities (Laruelle et al., 2003). Moreover, in accordance with the concept of functional selectivity (Lawler et al., 1999; Urban et al., 2007), one might suggest that SERT activity varies throughout the brain, as mechanisms regulating serotonin uptake, such as SERT internalization, may differ across brain areas. According to the "use it or lose it" hypothesis, SERT internalization depends on the transport activity, with sustained SERT blockage leading to enhanced internalization (Steiner et al., 2008). Furthermore, recent mathematical models relate SERT down-regulation in projection areas to antidepressant treatment response (Best et al., 2011), which is in accordance with recent SERT occupancy studies (Smith et al., 2011) and highlights the potential clinical relevance of regional occupancy differences, especially when considering the different regional involvement of distinct dysfunctions in mood disorders (Hoflich et al., 2012).

A recent study by our group focused on the influence of SERT pretreatment binding and SERT occupancy levels on clinical outcome after SSRI intake by investigating potential predictors of treatment response (Lanzenberger et al., 2012). The present longitudinal study focused solely on occupancy data and aimed to further illuminate a regional differentiation of SERT occupancies within a more basic neuropharmacological approach. Firstly, we aimed to investigate whether SERT occupancy is equally distributed in the brain in vivo using [^{11}C]DASB in depressed subjects (Q1). Based on information gleaned from animal research supporting scenario 2 (Kugelberg et al., 2001) and previous human findings opening the possibility of scenario 3, we hypothesized that SERT occupancy varies across regions (Meyer et al., 2004). A second objective was to substantiate differences in SERT occupancies between acute and chronic intake of SSRIs (Q2). As chronic SERT blockage was shown to down-regulate SERT cell surface expression (Benmansour et al., 1999), we hypothesized greater SERT occupancies after chronic SSRI intake. In order to further test the validity of the three different scenarios, we thirdly aimed to determine a potential relationship between baseline SERT expression and its change after treatment, i.e., SERT occupancy (Q3). Finally, we aimed to clarify the association between regional SERT occupancies and SSRI plasma levels (Q4). In accordance with Smith et al. (Smith et al., 2011) we adopted both a region of interest (ROI) and a voxel-wise approach, hereby allowing our study to benefit from the robustness and low disposition to noise attributed to ROI analysis, as well as a more detailed differentiation of occupancy through utilization of a voxel-wise processing of the PET data.

Methods

Participants

Nineteen out-patients suffering from major depression (13 females, 42.3 ± 7.8 years (mean ± sd)) were included in this study, as has been previously described (Lanzenberger et al., 2012). Subject assessment included a Structured Clinical Interview (SCID) for DSM IV and the 17 item Hamilton Depression Rating Scale (HAM-D), physical and neurological examinations, routine blood tests, an electrocardiogram and a pregnancy test. Inclusion criteria were a HAM-D score of ≥16, no comorbid axis II disorder, major medical or neurological illness, no intake of antidepressant agents or other substances with high affinity for SERT for three months prior to scanning (four months for fluoxetine), no history of drug abuse and no prior electroconvulsive and transcranial magnetic stimulation therapy. For demographic and clinical variables, see Table 1. All subjects gave written informed consent after detailed description of the study protocol. The study was approved by the Ethics Committee of the Medical University of Vienna.

Study design

Designed as a pooled longitudinal study, subjects received oral doses of either escitalopram (10 mg/day, 10 subjects) or citalopram (20 mg/day, 9 subjects) (Lundbeck A/S, Denmark), as previously described (Lanzenberger et al., 2012). Since no significant differences in SERT occupancy between citalopram and escitalopram were observed in an initial analysis (see Regional serotonin transporter occupancies (Q1) section), the data was pooled for further analysis in order to increase statistical power. Briefly, patients underwent three [^{11}C]DASB PET scans: before treatment (PET 1), 6 h following the first SSRI dose (PET 2) and 6 h after the last dose, which was administered daily for a minimum of 3 weeks (24.73 ± 3.3 days, PET 3).

Serum sampling

Blood samples were taken approximately 10 min before each PET scan and plasma was immediately separated by an experienced clinician. Plasma was then frozen at −20 °C and citalopram as well as S-citalopram analysis of the plasma fraction was undertaken by Quintiles Bioanalytical Laboratory, Uppsala, Sweden (www.analytical-services.se).

Positron emission tomography (PET)

PET scans were performed at the Department of Nuclear Medicine, Medical University of Vienna with a GE Advance full-ring scanner (General Electric Medical Systems, Milwaukee, WI, USA) in 3D mode. Following a 5 min transmission scan using retractable ^{68}Ge rod sources for tissue attenuation correction, data acquisition started simultaneously with a bolus injection of [^{11}C]DASB. Brain radioactivity was measured in a series of 30 consecutive time frames with 90 min total acquisition time divided into fifteen 1 min frames and fifteen 5 min frames. Collected data were reconstructed in volumes consisting of 35 trans-axial sections (128 × 128 matrix) using an iterative filtered back-projection algorithm (FORE-ITER) with a spatial resolution of 4.36 mm full-width at half maximum 1 cm next to the center of the field of view. For radiotracer preparation and radiochemical variables, see (Haeusler et al., 2009; Lanzenberger et al., 2012).

Table 1
Demographic and clinical variables.

Pat. no.	Age[a]	Sex	HAM-D			Duration of disease	Duration of current episode	Drug status	Drug[b]	Plasma Escit$_{ng/mL}$		Plasma Rcit$_{ng/mL}$	
			PET1	PET2	PET3					PET2	PET3	PET2	PET3
1	39	F	16	16	9	8 weeks	8 weeks	N	Cit	7.17	6.50	8.52	19.90
2	54	F	26	23	11	>10 years	>1 year	N	Cit	7.77	15.30	8.50	32.00
3	50	M	18	18	11	6 years	12 weeks	F	Cit	7.81	26.40	8.29	32.50
4	35	F	25	21	17	>1 year	8 weeks	F	Escit	10.40	26.00	<1.00	<1.00
5	28	F	19	19	8	>1 year	12 weeks	F	Cit	8.52	21.60	8.68	32.50
6	45	F	22	22	13	>10 years	>1 year	N	Escit	6.78	11.70	<1.00	<1.00
7	27	M	17	18	5	3 years	3 years	N	Escit	5.11	6.61	<1.00	<1.00
8	44	M	26	18	13	7 years	>2 weeks	F	Escit	5.74	12.90	<1.00	<1.00
9	46	F	16	16	3	>3 years	>2 years	F	Escit	<1.00	16.60	<1.00	<1.00
10	38	F	19	19	3	>1 year	>8 weeks	F	Escit	5.41	10.20	<1.00	<1.00
11	51	M	14	18	11	2.5 years	2.5 years	N	Escit	5.87	6.28	<1.00	<1.00
12	36	F	22	25	5	>1 year	2 weeks	F	Cit	8.84	20.00	9.46	24.60
13	42	M	16	16	17	>10 years	>6 months	F	Cit	5.31	8.95	6.48	17.40
14	47	F	24	9	9	>7 years	2 years	F	Cit	11.70	15.70	14.80	38.50
15	52	F	24	22	13	6 months	6 months	N	Cit	7.37	11.70	8.08	20.20
16	41	F	18	20	5	>10 years	3 weeks	N	Escit	6.50	16.90	<1.00	<1.00
17	52	F	25	19	4	2 years	2 years	N	Cit	7.88	19.40	8.67	32.90
18	38	M	18	11	13	6 months	6 months	N	Escit	6.50	13.30	<1.00	<1.00
19	38	F	19	19	2	>1 year	4 weeks	N	Escit	5.75	14.40	<1.00	<1.00

HAM-D: Hamilton Rating Scale for Depression.
Drug status: N, drug-naïve; F, drug-free.
[a] Age at PET 1.
[b] Daily dose for escit (escitalopram) was 10 mg, and for cit (citalopram) was 20 mg.

Serotonin transporter quantification and regions of interest

Following between-frame motion correction, individual summed PET images where spatially normalized to a PET template in stereotactic Montreal Neurological Institute (MNI) space using SPM8 (Wellcome Trust Centre for Neuroimaging, London, UK; http://www.fil.ion.ucl.ac.uk/spm/). Quantification of the SERT binding potential (BP_{ND}) (Innis et al., 2007) was done using the multilinear reference tissue model (MRTM2, Ichise et al., 2003). This model has been proven to be a useful method for human [^{11}C]DASB PET imaging and allows a rapid generation of parametric images of the SERT binding potential (Ichise et al., 2003), see Smith et al. (2011) for a comparison of results when using [^{11}C]DASB and different quantification methods. Cerebellar gray matter (excluding vermis and venous sinus) was used as reference region as recent post mortem and in vivo SERT quantification identified the cerebellar gray matter as optimal reference region for [^{11}C]DASB (Meyer, 2007; Parsey et al., 2006). All modeling calculations were performed using PMOD image analysis software, version 3.3 (PMOD Technologies Ltd, Zurich, Switzerland, www.pmod.com). SERT BP_{ND} was computed voxel-wise as well as in a ROI based approach. 22 ROIs were selected including subcortical structures such as the midbrain raphe nuclei, caudate, putamen and thalamus as well as cortical regions with moderate to higher SERT binding such as the cingulate and temporal cortex (see Table 2 and Fig. 1 for the list of selected ROIs).

Table 2
Regional SERT occupancy levels in 14 cortical and 8 subcortical regions of interest compared to mean cortical and subcortical SERT occupancies, respectively. *p < 0.05 Bonferroni corrected.
SERT, serotonin transporter.

	PET 2				PET 3			
	Mean	SD	t	p	Mean	SD	t	p
Cortical ROI								
Middle temporal gyrus	43.53	18.09	−5.19	<**0.001***	41.84	18.34	−5.09	**0.003***
Inferior temporal gyrus	47.40	20.67	−3.76	**0.011***	43.53	20.65	−4.17	**0.018***
Precuneus	58.50	18.43	−1.76	>0.1	50.10	26.49	−2.14	**0.036***
Superior temporal gyrus	60.54	16.08	−1.35	>0.1	54.83	22.16	−1.72	>0.1
Insula	64.54	11.12	−0.44	>0.1	66.08	13.86	0.71	>0.1
Orbitofrontal cortex	66.12	16.50	0.12	>0.1	65.69	14.70	0.54	>0.1
Cuneus	67.21	16.85	0.37	>0.1	67.56	20.82	0.74	>0.1
Gyrus rectus	67.44	11.65	0.67	>0.1	68.59	15.19	1.37	>0.1
Superior medial frontal cortex	68.53	18.33	0.61	>0.1	66.28	23.78	0.37	>0.1
Medial cingulate	70.53	12.41	1.67	>0.1	66.26	20.28	0.52	>0.1
Calcarine gyrus	71.45	16.14	1.52	>0.1	67.68	15.76	1.01	>0.1
Anterior cingulate	72.80	20.70	1.50	>0.1	72.34	14.12	2.56	**0.045***
Posterior cingulate	78.49	11.65	4.12	>0.1	78.55	16.27	3.51	**0.002***
Subgenual cingulate	82.16	7.36	9.51	**0.006***	84.12	9.16	9.14	**0.013***
Subcortical ROI								
Hippocampus	65.01	15.33	−2.27	>0.1	70.06	15.90	−2.26	>0.1
Putamen	66.71	5.27	−5.19	<**0.001***	71.10	6.32	−5.12	<**0.001***
Thalamus	67.92	6.46	−3.42	<**0.001***	73.83	6.72	−3.05	**0.001***
Olfactory bulb	70.40	8.14	−1.39	>0.1	74.84	8.67	−1.86	**0.012***
Caudate	72.10	5.14	−0.76	>0.1	77.00	6.42	−1.04	>0.1
Median raphe	78.14	6.16	3.641	**0.012***	85.13	4.75	6.04	**0.004***
Amygdala	81.78	6.48	5.909	<**0.001***	87.58	6.74	5.69	<**0.001***
Dorsal raphe	81.88	4.52	8.57	<**0.001***	88.78	3.56	12.56	<**0.001***

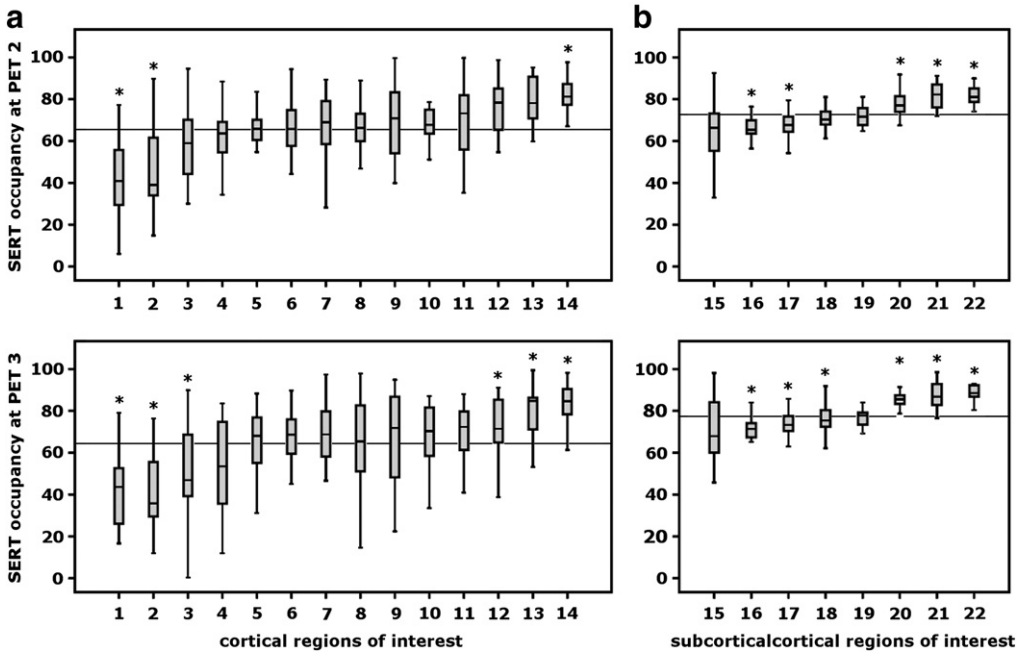

Fig. 1. Boxplots representing differential regional SERT occupancies after single dosage (PET 2, upper row) and steady state (PET 3, bottom row) SSRI intake when tested against mean occupancy values for (*a*) cortical and (*b*) subcortical regions. Significant regional SERT occupancy deviations from the mean (horizontal line within each boxplot) are indicated by an asterisk (see Table 2 for means, SD and t-values). Numbers on the x-axis indicate the selected regions of interest ordered by mean occupancy strength: *1* middle temporal gyrus; *2* inferior temporal gyrus; *3* precuneus, *4* superior temporal gyrus, *5* insula, *6* orbitofrontal gyrus, *7* cuneus, *8* gyrus rectus, *9* superior medial frontal cortex, *10* medial cingulate, *11* calcarine gyrus, *12* anterior cingulate, *13* posterior cingulate, *14* subgenual cingulate, *15* hippocampus, *16* putamen, *17* thalamus, *18* olfactory bulb, *19* caudate, *20* median raphe nucleus, *21* amygdala, *22* dorsal raphe nucleus. SERT, serotonin transporter; SSRI, selective serotonin reuptake inhibitor; PET, positron emission tomography; SD, standard deviation.

Only regions and voxels with residual SERT $BP_{ND} \geq 0.05$ were included in subsequent analyses to avoid spurious occupancy values due to the low signal-to-noise ratio in these regions. For similar reasons, only ROIs and voxels that showed a decrease in SERT BP_{ND} over time were included. Given that SSRIs are defined by blocking the SERT, only occupancy values ≥ 0 should reflect accurate drug occupancies (for description of increased SERT BP_{ND} over time, i.e., negative occupancy values, see supplementary Table A5). SERT occupancy was derived using the equation: Occupancy (%) $= (1 - BP_{ND}$ treatment$/BP_{ND}$ baseline$) \times 100$. In order to avoid bias induced by manual delineation, ROIs (except for dorsal, DRN and median raphe nucleus, MRN) were taken from a standardized ROI atlas (Fink et al., 2009; Stein et al., 2008) based on the automated anatomical labeling (AAL) brain atlas (Tzourio-Mazoyer et al., 2002). SERT binding in the DRN and MRN was defined manually in two slices of the template comprising spheres of 3 mm radius (Kranz et al., 2012).

Statistical analysis

To assess whether SERT occupancies show regional differences (Q1), regional occupancy values were compared to a mean occupancy across regions. This was performed separately for cortical and subcortical ROIs. Repeated-measures ANOVA was performed using medication (escitalopram vs. citalopram) as between subjects factor and ROI including a "mean ROI" as the within subjects factor. Post hoc paired samples t-tests were performed in order to test ROI values against the mean of regional occupancies. Furthermore, a paired samples *t*-test was performed to compare the mean of cortical to the mean of subcortical ROIs. To assess Q1 within the voxel-wise approach, one sample t-tests were used, as provided in SPM software. Assessment of differences between SERT occupancies at PET 2 and PET 3 (Q2) for both the ROI- and voxel-based approach was done using repeated-measures ANOVA with time and either ROI or voxel (PET 2 and PET 3) as factors. Next, we assessed if SERT occupancies depend on pretreatment SERT binding (Q3). Simply correlating these two variables would produce a well-known statistical artifact, as correlations of any pretreatment value with changes of these values over time are mathematically inevitable (Gill et al., 1985). Two different approaches were adopted to solve this problem. First, regression analysis that predicted residual SERT BP_{ND} (PET 2 and 3, respectively) from baseline SERT BP_{ND} was computed. Second, correlation analysis between absolute SERT reduction and Oldham's transformation, i.e., (baseline BP_{ND} + residual BP_{ND})/2 (Oldham, 1962) was performed. Thus, while the first approach assesses the relationship between baseline and residual SERT BP_{ND}, the second approach gives an unbiased correlation between baseline SERT BP_{ND} and its change after treatment (Tu and Gilthorpe, 2007). Both approaches were performed for each ROI and voxel to assess the strength of associations for a defined brain region (subjects as single values). In a second step, means of ROIs were entered into the analyses as single values to assess the strength of associations across the brain (ROIs as single values). Finally, to test whether individual SERT occupancies depend on escitalopram plasma levels (Q4), Pearson correlation was performed for each ROI and voxel. Correction for multiple comparisons was done using Bonferroni and family-wise error rate (FWE), for ROI and voxel-wise analyses, respectively. SPSS version 18.0 for Windows (SPSS Inc., Chicago, IL, www.spss.com) was used for computation within the ROI-based approach. Voxel-wise analysis was done using MATLAB and SPM8.

Results

Sample characteristics

Most subjects benefited from treatment, with eleven out of nineteen subjects being responders (showing at least a 50% reduction in HAM-D scores) and seven of these becoming remitters with final HAM-D scores ≤ 7, see Table 1 or Lanzenberger et al. (2012) for more details. Serum concentrations for active moieties (+)-citalopram and (−)-citalopram are shown in Table 1. Escitalopram plasma levels increased significantly from 7.25 ± 1.79 ng/mL at PET 2 to 14.76 ± 6.02 ng/mL at PET 3

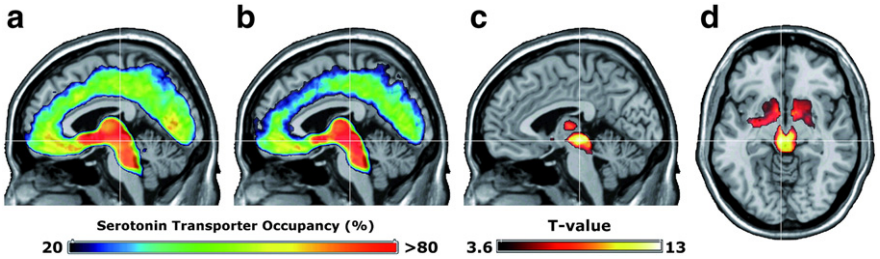

Fig. 2. Sagittal views of voxel-wise maps representing the averaged SERT occupancies after *(a)* single dosage (PET 2) and *(b)* steady state (PET 3) escitalopram or citalopram intake, overlaid onto structural MRI planes. Occupancy values are given in the color table. *(c)* and *(d)* show increased SERT occupancies at PET 3 compared to PET 2. Significant clusters are restricted to basal ganglia, thalamus and midbrain, $p < 0.05$ corrected, $k > 5$ voxels. Crosshair at −4/−23/−8 mm. Left is left. SERT, serotonin transporter; PET, positron emission tomography.

($p < 0.001$, paired sample t-test). Likewise, citalopram levels increased significantly from 9.05 ± 2.30 ng/mL at PET 2 to 27.83 ± 7.42 ng/mL at PET 3. Injected doses and specific activities for [^{11}C]DASB did not significantly differ between PET measurements (data not shown).

Regional serotonin transporter occupancies (Q1)

ROI based occupancy values approximately six hours following the first SSRI dose (PET 2) ranged between 43.53 ± 18.09% (minimum regional SERT occupancy in the middle temporal gyrus) and 82.16 ± 7.36% (maximum regional SERT occupancy in the subgenual cingulate cortex, sgCC). Mean cortical occupancy values were significantly lower than mean subcortical occupancy values (65.66 ± 10.60% vs. 72.99 ± 6.75%, $p = 0.001$, paired sample t-test). For cortical occupancies, repeated-measures ANOVA revealed a significant main effect of ROI ($F_{14,140} = 16.39$, $p < 0.001$) but neither a main effect of medication intake ($F_{1,10} = 0.001$, $p > 0.1$) nor an interaction effect ($F_{14,140} = 0.92$, $p > 0.1$). Post-hoc paired sample t-tests revealed that middle and inferior temporal cortex had significantly lowered occupancies, whereas sgCC had significantly greater occupancies compared to mean cortical occupancies ($p < 0.05$, corrected). Likewise, for subcortical regions, there was a significant main effect of ROI ($F_{8,136} = 26.79$, $p < 0.001$) but no main effect of medication intake ($F_{1,17} = 0.04$, $p > 0.1$) and no interaction effect ($F_{8,136} = 0.18$, $p > 0.1$). Post-hoc paired sample t-tests revealed that subcortical regions such as the putamen and thalamus, exhibited decreased occupancies, whereas amygdala, DRN and MRN had greater occupancy values compared to mean subcortical occupancies (see Table 2, for regional occupancies of the two medications, see Table A1).

Results were mostly reflected within the voxel-wise approach, showing greater cortical occupancies within clusters extending to the sgCC and inferior orbitofrontal cortex and lowered cortical occupancies in temporal but also frontal, parietal and occipital regions. Analogous results within the voxel-wise analyses were also observed for subcortical regions. Interestingly, the voxel-wise approach also revealed occupancy differences within a single anatomical region. Whereas occupancy was greater within a ventral posterior part of the thalamus, a more anterior part showed significantly lowered occupancies bilaterally (for a complete list of corrected and uncorrected values, see Table 3.1).

Similar data were obtained when investigating SERT occupancy after three weeks of treatment (PET 3). Regional occupancy values ranged between 41.84 ± 18.34% and 84.12 ± 9.16%. Mean cortical occupancies

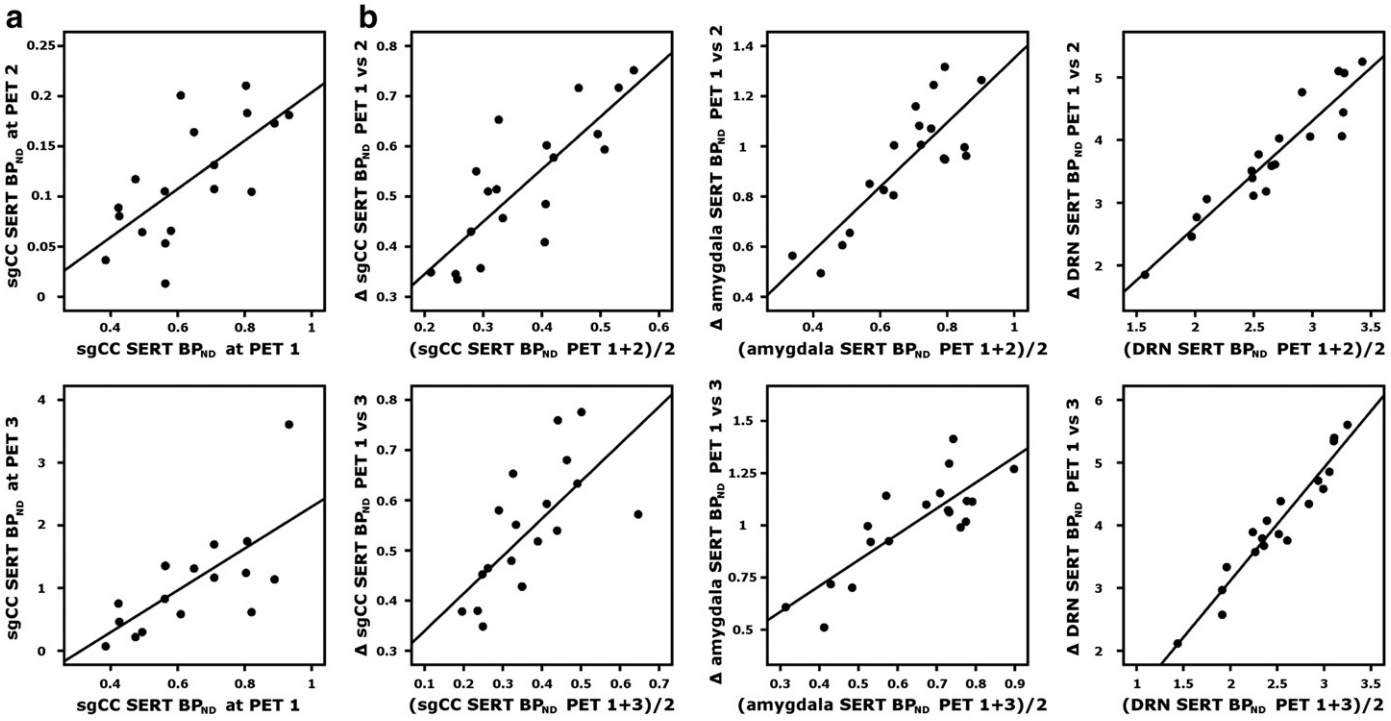

Fig. 3. Prediction of residual SERT binding and steepness of SERT decline at PET 2 (upper row) and PET 3 (bottom row) by pretreatment SERT binding. *(a)* Scatter plots representing the association between pretreatment and residual SERT binding in the sgCC. *(b)* Association between the mean of pretreatment and residual SERT binding and absolute reduction of SERT binding in the sgCC, amygdala and DRN. SERT, serotonin transporter; PET, positron emission tomography; sgCC, subgenual cingulate cortex; DRN, dorsal raphe nuclei.

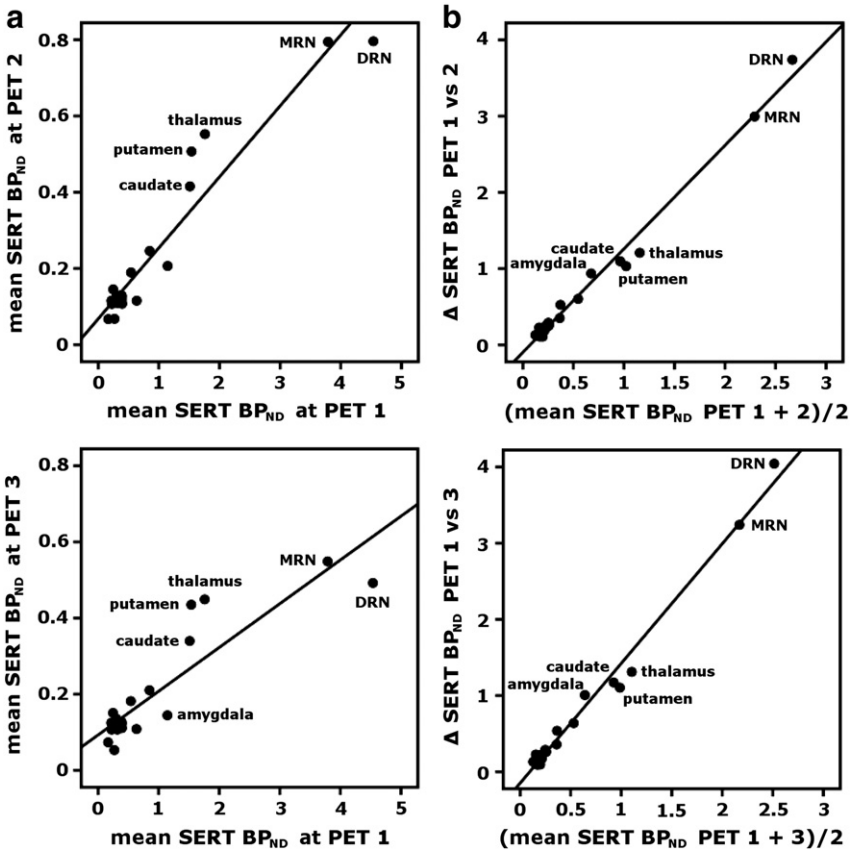

Fig. 4. Scatter plots representing the association between *(a)* regional SERT pretreatment binding and residual binding and between *(b)* the mean of pretreatment and residual SERT binding and absolute reduction of SERT binding at PET 2 (upper row) and PET 3 (bottom row). Dots represent mean values for each region across subjects. SERT, serotonin transporter; PET, positron emission tomography.

were significantly lower than mean subcortical occupancies (63.82 ± 12.21% vs. 78.54 ± 7.52%, $p < 0.001$, paired sample t-test). For cortical regions, repeated-measures ANOVA revealed a significant main effect of ROI ($F_{14,98} = 26.47$, $p < 0.001$) but no main effect of medication intake ($F_{1,7} = 0.29$, $p > 0.1$) and no interaction effect ($F_{14,98} = 1.17$, $p > 0.1$). Post-hoc paired sample t-tests revealed that middle and inferior temporal cortex as well as precuneus had significantly lowered occupancies, whereas anterior, posterior (PCC) and subgenual cingulate cortex (sgCC) had significantly greater occupancies compared to mean cortical occupancies ($p < 0.05$, corrected). For subcortical regions, there was a significant main effect of ROI ($F_{8,128} = 28.09$, $p < 0.001$) but no main effect of medication intake ($F_{1,16} = 0.46$, $p > 0.1$) and no interaction effect ($F_{8,128} = 0.60$, $p > 0.1$). Post-hoc paired sample t-tests revealed that the putamen, thalamus and olfactory bulb exhibited decreased occupancies, whereas amygdala, DRN and MRN had greater occupancies compared to the mean subcortical occupancy (see Table 2 and Table A1). Similarly, the voxel-wise computation revealed significantly lowered SERT occupancies for bilateral middle temporal gyrus and putamen, and greater occupancy for the midbrain. Additionally, deviating SERT occupancies from the mean subcortical occupancy were detected for the left and right thalamus. The elevated occupancy values in the PCC and sgCC revealed in the ROI-based approach could not be replicated in the voxel-wise approach (see Table 3.2 for a complete list of corrected and uncorrected values).

Serotonin transporter occupancies after acute and prolonged intake of SSRIs (Q2)

Repeated-measures ANOVA with ROI and time (PET 2 and PET 3) as factors revealed a main effect of ROI ($F_{(21,168)} = 27.558$, $p < 0.001$) but no main effect of time. Additionally, a significant ROI by time interaction ($F_{(21,168)} = 3.627$, $p < 0.001$) was present, with *post-hoc* comparisons suggesting changes in occupancy over time in some but not in all brain regions: an increased occupancy after three weeks of treatment was seen only in subcortical regions (see Fig. 2), namely in DRN ($T = -9.215$, $p < 0.001$) and MRN ($T = -6.297$, $p < 0.001$), the amygdala ($T = -3.806$, $p = 0.001$) and thalamus ($T = -4.885$, $p < 0.001$, all $p < 0.05$ corrected), as well as a statistical trend in the caudate ($T = -3.118$, $p = 0.006$). These results were mostly confirmed by the voxel-wise analysis, revealing significant clusters restricted to the midbrain raphe nuclei ($T = 12.61$, 2/−22/−8 mm (x/y/z)), caudate ($T = 11.49$, −6/2/−8 mm) and bilateral thalamus ($T = 9.72$, 2/−14/6 mm, $T = 8.37$, −8/−22/4 mm, $p < 0.05$ corrected, $k > 5$ voxels).

Predictors of serotonin transporter occupancies (Q3 and Q4)

Assessing the predictive value of pretreatment SERT binding on residual binding for each brain region (at PET 2 and PET 3) revealed a positive association only for the sgCC (PET 2: $R^2 = 0.43$, $\beta = 0.68$, $T = 3.73$, $p < 0.05$ corrected; PET 3: $R^2 = 0.45$, $\beta = 0.7$, $T = 3.74$, $p < 0.05$ corrected), as well as a borderline significance for the hippocampus (PET 3, $R^2 = 0.41$, $\beta = 0.67$, $T = 3.6$, $p = 0.002$, uncorrected) and trends for orbitofrontal cortex and anterior cingulate (see Table A2 for a list of corrected and uncorrected values). Interestingly, voxel-wise analysis revealed partially different results. For PET 2, peak associations were found in the right caudate ($T = 9.39$, $R^2 = 0.83$, 14/24/-2 mm); right anterior cingulate ($T = 8.74$, $R^2 = 0.81$, 14/32/26 mm) and left temporal pole ($T = 7.24$, $R^2 = 0.75$, −38/8/−20 mm) whereas for PET 3, associations were present in the sgCC ($T = 8.70$, $R^2 = 0.81$, 2/20/−4 mm), right temporal pole ($T = 8.55$, $R^2 = 0.80$, 40/

Table 3.1
Regional SERT occupancy levels compared to mean cortical and subcortical SERT occupancies at PET 2 following a voxel-wise approach. *p < 0.05 FWE corrected voxel-level, p < 0.001 uncorrected voxel-level, cluster extent threshold k > 5 voxel, MNI coordinates in mm, L left, R right. SERT, serotonin transporter; PET, positron emission tomography; FWE, family wise error; MNI, Montreal Neurological Institute.

Anatomical region (AAL)	MNI coordinates						
	BA	x	y	z	t	p	Cluster size
Regional occupancy > mean cortical occupancy at PET 2							
Inferior orbitofrontal cortex L	38	−24	16	−20	8.37	<**0.001***	41
Subgenual cingulate cortex L	11	−2	30	−10	6.29	<0.001	–
Lingual gyrus L	19	−16	−50	−4	5.82	<0.001	24
Middle cingulate r	24	4	14	32	5.76	<0.001	93
Parahippocampal gyrus L	35	−20	−18	−22	5.28	<0.001	7
Heschl gyrus R	48	38	−20	12	4.75	<0.001	30
Middle cingulate gyrus	23	0	−18	34	4.52	<0.001	10
Anterior cingulate L	24	−6	32	20	4.46	<0.001	22
Anterior cingulate	24	0	36	12	4.35	<0.001	17
Superior temporal gyrus L	48	−42	0	−12	4.11	<0.001	7
Middle cingulate L	23	−2	−4	38	4.03	<0.001	9
Regional occupancy < mean cortical occupancy at PET 2							
Middle temporal gyrus R	37	44	−70	14	12.24	<**0.001***	4576
Middle frontal gyrus L	46	−34	52	20	8.87	<**0.001***	1865
Middle temporal gyrus L	37	−56	−54	4	8.62	<**0.001***	5100
Middle orbitofrontal gyrus R	11	28	60	−8	7.75	<**0.001***	1070
Precuneus R	7	6	−70	48	6.46	<0.001	537
Inferior triangular frontal gyrus L	45	−46	24	4	6.20	<0.001	256
Cuneus R	–	6	−70	28	5.44	<0.001	90
Precuneus L	–	−8	−50	36	4.93	<0.001	22
Inferior triangular frontal gyrus L	44	−38	16	32	4.62	<0.001	33
Parahippocampal gyrus R	20	30	−30	−12	4.61	<0.001	15
Middle frontal gyrus R	6	36	−2	58	4.61	<0.001	35
Insula R	48	46	10	6	4.50	<0.001	39
Inferior triangular frontal gyrus R	48	42	20	30	4.41	<0.001	8
Insula R	48	42	18	4	4.34	<0.001	29
Superior orbitofrontal cortex L	11	−14	36	−20	4.32	<0.001	8
Middle frontal gyrus L	46	−36	28	40	4.29	<0.001	11
Middle frontal gyrus L	8	−26	28	50	4.26	<0.001	31
Precentral gyrus L	6	−34	0	62	4.26	<0.001	16
Fusiform gyrus R	19	26	−62	10	4.24	<0.001	8
Precentral gyrus R	44	44	10	34	4.11	<0.001	27
Inferior occipital gyrus L	18	−28	−90	−10	4.10	<0.001	12
Precuneus R	7	2	−68	56	4.09	<0.001	6
Precentral gyrus L	6	−42	2	48	3.95	<0.001	6
Inferior orbitofrontal cortex R	47	38	40	−8	3.95	<0.001	7
Regional occupancy > mean subcortical occupancy at PET 2							
Midbrain (tectum)	–	2	−30	−4	14.35	<**0.001***	952
Midbrain (DRN)		0	−26	−6	13.41	<**0.001***	–
Thalamus R	–	6	−28	4	8.56	<**0.001***	
Amygdala L	34	−20	0	−20	8.10	<**0.001***	107
Caudate R	–	8	14	0	7.86	<**0.001***	–
Amygdala R	35	14	−8	−16	7.56	<0.001	109
Caudate L	–	−12	8	10	5.63	<0.001	–
Pons L	–	−6	−26	−32	5.12	<0.001	14
Regional occupancy < mean subcortical occupancy at PET 2							
Thalamus R	–	−12	−10	6	10.43	<**0.001***	–
Thalamus L	–	10	−14	4	9.16	<**0.001***	–
Putamen R	–	−10	−22	−14	8.98	<**0.001***	–
Putamen L	–	10	−24	−14	7.34	<0.001	–
Amygdala R	–	34	4	0	6.27	<0.001	–
Hippocampus L	–	−28	4	−4	5.81	<0.001	–

Table 3.2
Regional SERT occupancy levels compared to mean cortical and subcortical SERT occupancies at PET 3 following a voxel-wise approach. *p < 0.05 FWE corrected voxel-level, p < 0.001 uncorrected voxel-level, cluster extent threshold k > 5 voxel, MNI coordinates in mm, L left, R right. SERT, serotonin transporter; PET, positron emission tomography; FWE, family wise error; MNI, Montreal Neurological Institute.

Anatomical region (AAL)	MNI coordinates						
	BA	x	y	z	t	p	Cluster size
Regional occupancy > mean cortical occupancy at PET 3							
Middle cingulate gyrus L	24	−4	2	40	6.66	<0.001	154
Lingual gyrus R	17	2	−80	4	5.57	<0.001	87
Lingual gyrus L	18	−14	−56	−2	5.31	<0.001	36
Calcarine gyrus	17	0	−84	0	4.93	<0.001	7
Fusiform gyrus L	30	−28	−22	−28	4.57	<0.001	6
Superior temporal pole L	38	−40	20	−28	4.53	<0.001	8
Supplementary motor area L	6	−8	−16	56	4.39	<0.001	6
Anterior cingulate L	24	−6	30	22	4.35	<0.001	15
Lingual gyrus R	18	14	−56	−4	4.31	<0.001	6
Supplementary motor area R	–	6	−4	50	4.15	<0.001	13
Anterior cingulate R	24	6	26	24	3.96	<0.001	6
Middle cingulate gyrus R	24	6	12	36	3.95	<0.001	10
Regional occupancy < mean cortical occupancy at PET 3							
Middle temporal gyrus R	37	54	−58	16	10.68	<**0.001***	3860
Middle temporal gyrus L	37	−54	−60	16	9.16	<**0.001***	4708
Middle frontal gyrusL	10	−30	62	0	6.95	<0.001	1287
Middle frontal gyrus R	46	36	54	14	6.22	<0.001	618
Inferior frontal operculum L	48	−48	12	0	6.06	<0.001	311
Superior frontal gyrus L	10	−18	50	10	4.75	<0.001	18
Precuneus R	–	10	−48	50	4.56	<0.001	18
Precuneus L	–	−8	−58	34	4.63	<0.001	68
Middle frontal gyrus L	46	−20	46	18	4.63	<0.001	7
Rolandic operculum R	48	52	10	6	4.58	<0.001	30
Inferior frontal operculum R	44	42	16	30	4.51	<0.001	26
Precentral gyrus L	6	−40	0	50	4.45	<0.001	12
Fusiform gyrus R	20	44	−28	−26	4.41	<0.001	12
Middle frontal gyrus R	6	30	−2	56	4.38	<0.001	9
Middle frontal gyrus R	45	42	30	32	4.34	<0.001	12
Superior orbitofrontal cortex L	11	−14	64	−12	4.32	<0.001	9
Precuneus L	–	−2	−70	34	4.31	<0.001	28
Cuneus R	–	8	−70	28	4.24	<0.001	9
Precuneus R	–	6	−66	50	4.21	<0.001	16
Precuneus L	–	−6	−66	50	4.19	<0.001	17
Inferior frontal operculum R	48	42	12	8	4.14	<0.001	28
Middle frontal gyrus R	8	30	24	44	4.00	<0.001	8
Regional occupancy > mean subcortical occupancy at PET 3							
Midbrain (tectum)	–	0	−30	−6	15.21	<**0.001***	888
Thalamus R	–	8	−30	2	7.21	<0.001	–
Caudate L	–	−6	14	−6	6.85	<0.001	–
Caudate R	–	10	16	0	5.76	<0.001	–
Midbrain (median raphe nucleus)	–	0	−32	−18	4.62	<0.001	8
Regional occupancy < mean subcortical occupancy at PET 3							
Thalamus R	–	12	−14	2	13.76	<**0.001***	–
Thalamus L	–	−12	−12	6	12.14	<**0.001***	–
Putamen R	–	32	12	4	9.42	<**0.001***	–
Putamen L	–	−30	4	6	8.12	<**0.001***	–
Amygdala R	–	34	−2	−22	5.38	<0.001	17
Hippocampus L	–	−24	−10	−22	4.65	<0.001	–

12/−30 mm) and left middle occipital cortex (T = 7.72, R^2 = 0.77, −44/−64/2 mm, all p < 0.05 corrected, k > 5 voxels). That is, subjects with higher pretreatment SERT binding in these regions also had significantly higher residual SERT binding after treatment.

Assessing the association between the mean of baseline and residual SERT binding (Oldham's transformation) and absolute change after treatment within the ROI-based approach revealed highly significant positive correlations for both PET 2 and PET 3 in most subcortical regions, as well as the PCC and sgCC (all p < 0.05 corrected, see Table 4 and Fig. 3). Correlations were confirmed within the voxel-wise approach (see Table A3 for a complete list of corrected and uncorrected values). These results therefore represent a strong and unbiased test for differential baseline effects of SERT BP_{ND} on change after both acute and prolonged SSRI treatment in these regions.

Regression analysis across the brain using ROI means as single values revealed a strong positive effect of pretreatment SERT binding on residual SERT binding at PET 2 (R^2 = 0.92, β = 0.96 T = 15.10, p < 0.001) and PET 3 (R^2 = 0.80, β = 0.89 T = 8.94, p < 0.001). Thus, when averaged across subjects, regions with higher SERT binding before

Table 4
Correlation analysis between absolute SERT reduction and Oldham's transformation at PET 2 and PET 3 (baseline BP_{ND} + residual BP_{ND})/2 in 22 regions of interest. *p < 0.05 Bonferroni corrected. SERT, serotonin transporter; PET, positron emission tomography; BP_{ND}, non-displaceable binding potential.

ROI	PET 2		PET 3	
	r	p	r	p
Middle temporal gyrus	0.03	0.894	0.14	0.563
Inferior temporal gyrus	0.16	0.523	0.01	0.978
Precuneus	0.37	0.119	0.34	0.160
Superior temporal gyrus	0.30	0.205	0.08	0.747
Insula	0.62	0.005	0.39	0.102
Orbitofrontal cortex	0.47	0.044	0.43	0.066
Cuneus	0.48	0.036	0.41	0.078
Gyrus rectus	0.56	0.013	0.37	0.121
Superior medial frontal cortex	0.49	0.064	0.28	0.348
Medial cingulate	0.60	0.006	0.57	0.011
Calcarine gyrus	0.61	0.005	0.60	0.007
Anterior cingulate	0.54	0.016	0.64	0.003
Posterior cingulate	0.72	**0.001***	0.79	<**0.001***
Subgenual cingulate	0.81	<**0.001***	0.68	**0.002***
Hippocampus	0.49	0.035	0.23	0.345
Putamen	0.82	<**0.001***	0.83	<**0.001***
Thalamus	0.86	<**0.001***	0.82	<**0.001***
Olfactory bulb	0.80	<**0.001***	0.73	<**0.001***
Caudate	0.88	<**0.001***	0.82	<**0.001***
Median raphe	0.91	<**0.001***	0.93	<**0.001***
Amygdala	0.84	<**0.001***	0.83	<**0.001***
Dorsal raphe	0.94	<**0.001***	0.96	<**0.001***

treatment had higher residual SERT binding after approximately six hours and three weeks of treatment. Similarly, high associations were found between Oldham's transformation and absolute change after treatment across brain regions, revealing highly significant positive correlations for both PET 2 and PET 3 (both $r = 0.99$, $p < 0.001$). That is, regions with higher baseline SERT BP_{ND} were significantly more occupied/down-regulated by acute and prolonged SSRI treatment (see Fig. 4). Statistical assumptions of homoscedasticity and normal distribution of residuals were met.

Finally, correlation analysis between escitalopram plasma levels and occupancy at PET 2 revealed no significant associations for any ROI or voxel. In fact, such correlations were also not found at uncorrected levels. For PET 3, ROI analysis revealed significant correlations for caudate and putamen, thalamus and DRN ($P < 0.05$, corrected, see Table 5, see also Fig. 5). These results were confirmed by the voxel-wise analysis, showing clusters mostly restricted to the midbrain and diencephalon, with two clusters in the basal ganglia surviving FWE correction (see Table A4). These findings imply that individual plasma levels of escitalopram affect SERT occupancy after continuous treatment in the midbrain, thalamus and basal ganglia. However, they only marginally affect SERT occupancy after 6 h of drug intake.

Table 5
Correlation analysis between escitalopram plasma levels and SERT occupancy at PET 2 and PET 3 in 22 regions of interest. *p < 0.05 Bonferroni corrected. SERT, serotonin transporter; PET, positron emission tomography.

ROI	PET 2		PET 3	
	r	p	r	p
Middle temporal gyrus	0.05	0.828	0.55	0.018
Inferior temporal gyrus	0.08	0.753	0.52	0.027
Precuneus	0.45	0.081	0.44	0.077
Superior temporal gyrus	0.18	0.474	0.14	0.569
Insula	0.08	0.745	0.46	0.047
Orbitofrontal cortex	<0.01	0.998	0.21	0.412
Cuneus	0.34	0.204	0.11	0.686
Gyrus rectus	0.10	0.677	0.09	0.722
Superior medial frontal cortex	0.11	0.700	−0.02	0.956
Medial cingulate	0.18	0.489	0.49	0.034
Calcarine gyrus	0.22	0.388	0.31	0.234
Anterior cingulate	0.06	0.823	0.34	0.166
Posterior cingulate	0.26	0.365	0.35	0.207
Subgenual cingulate	0.26	0.303	−0.04	0.866
Hippocampus	0.24	0.320	0.03	0.907
Putamen	0.29	0.224	0.70	**0.001***
Thalamus	0.34	0.161	0.68	**0.001***
Olfactory bulb	0.15	0.540	0.59	0.008
Caudate	0.20	0.411	0.70	**0.001***
Median raphe	0.35	0.137	0.45	0.054
Amygdala	0.29	0.233	0.29	0.243
Dorsal raphe	0.34	0.161	0.71	**0.001***

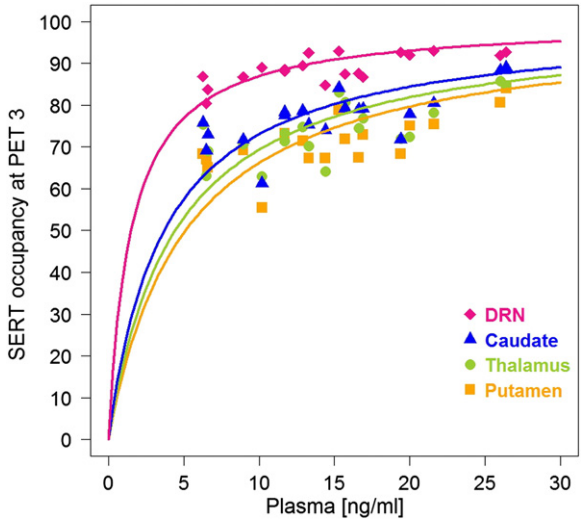

Fig. 5. Association between escitalopram plasma level and SERT occupancy at steady state treatment (PET 3) in the DRN (pink checkers), caudate (blue triangles), thalamus (green circles) and putamen (orange squares). Data were fitted by a hyperbolic curve of the form $f(x) = a*x/(b + x)$, where f(x) refers to occupancy and x refers to escitalopram plasma level. Data are mostly restricted to the upper half of the curve above the bend which is due to the administration of a constant dosage of 20 mg of citalopram and 10 mg of escitalopram, respectively. Therefore, data were further fitted using a linear relationship. We thus used Pearson product–moment correlation analysis to assess the association between plasma and occupancy (see methods). SERT, serotonin transporter; PET, positron emission tomography, DRN, dorsal raphe nucleus.

Discussion

In this longitudinal PET study, we investigated regional SERT occupancy after acute and after three weeks of citalopram and escitalopram treatment in patients with major depressive disorder. Our first research question (Q1) aimed to address whether SERT occupancy levels are equally distributed (corresponding to scenario 1) or spread differently among individual brain regions (scenario 2 or 3). We found that subcortical SERT occupancies were on average greater than cortical occupancies. Furthermore, within cortical ROIs, we found occupancy values to be greater in sgCC and lower in temporal cortex when compared to the mean cortical occupancy. For subcortical ROIs, we found greater occupancy in the amygdala, MRN and DRN, whereas thalamus and putamen exhibited lower occupancies compared to the mean subcortical occupancy (see Fig. 1, Tables 2 and 3.1 and 3.2).

With respect to the ROI based results, one might therefore detect an overall trend towards smaller ROIs showing greater occupancies. However, the voxel-based results, which mostly confirm the ROI analysis, make this methodological concern less probable, as voxel size did not differ throughout the brain. Further methodological considerations such as partial volume effects related signal decreases in small brain structures may be considered but seem equally unlikely, as signal underestimations should be similar for consecutive PET measurements and therefore barely affect occupancy values in a systematic manner.

When applying neuropharmacological explanations rather than the methodological interpretations addressed above, our data render

scenario 1 unlikely. As given in the equation from the introduction, SERT occupancy is proportional to the product of free drug concentration, SERT availability and SERT affinity. When assuming a brain-wide uniform affinity of the drugs and the radiotracer [^{11}C]DASB (Zeng et al., 2006) and given a topologically inhomogeneous SERT availability, suggests a variability in regional drug concentration and other factors not mentioned in this manuscript as possible causes for diverse SERT occupancies. Indeed, earlier animal studies found region specific variations in citalopram concentrations, supporting scenario 2. (Kugelberg et al., 2001; Kugelberg et al., 2003; Kugelberg et al., 2004), although see (Kingback et al., 2011). However, our results suggest that baseline SERT binding is positively correlated with SERT binding reduction (Q3, see Fig. 4), indicating that occupancy is higher in regions with higher SERT density, which is envisioned in scenario 3.

This is in line with pharmacological research, suggesting that in regions with high target density, drug molecules are more likely to rebind to the same target or targets nearby (Vauquelin and Charlton, 2010). Therefore, in a restricted diffusion model such as the living human brain, forward rates and reverse rates of the drug to and from its target, respectively, will be decelerated in regions with high target density. This is illustrated in equations

$$k_f = k_{on}/(1 + k_{on}N/k_+) \quad (2)$$

and

$$k_r = k_{off}/(1 + k_{on}N/k_-) \quad (3)$$

where k_f and k_r are the effective forward and reverse rate coefficients, k_{on} and k_{off} association and dissociation rate constants, N the amount of free targets available and k_+ and k_- the diffusion limited forward and reverse rate constants (Vauquelin and Charlton, 2010). Decelerated forward rates will also apply for the radioligand administered approximately 6 h after drug intake, leading to reduced radioligand binding and thus increased occupancy values in regions with high SERT density. Moreover, decelerated reverse rates of the drug may also affect forward rates of the administered radioligand, which further increases occupancy values. Finally, decelerated forward and reverse rates in regions with high SERT density may also translate to decelerated fluctuations in SERT occupancies and thus to smaller variance in regions with high SERT density, which is reflected by our data (see Fig. 1).

Differences in rate velocities may also explain the associations between baseline SERT binding and binding reduction beyond an expected regression towards the mean (Q3). Subjects with higher regional baseline SERT binding exhibited stronger SERT binding reduction, as assessed using Oldham's transformation. However, this association was present only in sgCC and subcortical regions (see Table 4 and Table A3, Fig. 3b), which, again, can be explained by decelerated fluctuations in SERT occupancies in these regions, whereas greater variances in regions with lower SERT densities may have destroyed such associations. Interestingly, when investigating the association between baseline and residual SERT binding, we only found significant results for the sgCC and statistical trends for hippocampus, anterior cingulate and orbitofrontal regions (see Table A2 and Fig. 3a). This indicates that pretreatment SERT availability seems to be related to both residual SERT availability and SERT blockage by citalopram/escitalopram only for the sgCC, a region that is known to be strongly involved in the treatment of mood disorders (Mayberg, 2009).

Interestingly, the issue of substance-specific regional binding selectivity has been largely discussed since the late 90s in the context of antipsychotics. In fact, the “atypicality” of certain agents, more specifically their antipsychotic features regarding negative and positive symptoms and the low occurrence of extrapyramidal side effects, has been attributed to a preferential mesolimbic compared to striatal binding (Grunder et al., 2006; Kegeles et al., 2008; Pilowsky et al., 1997; Vernaleken et al., 2008; Xiberas et al., 2001), although see (Grunder et al., 2008; Takahata et al., 2012) for aripiprazol. However, region specific occupancy differences are explained by regionally varying endogenous dopamine concentrations (Grunder et al., 2006; Seeman, 2002) and the different kinetics of dopamine release and reuptake across brain regions (Garris and Wightman, 1994).

The second hypothesis of the present study concerns the comparison of SERT occupancies after acute and continuous SSRI treatment (Q2). We found significantly greater SERT occupancy in subcortical regions including the midbrain raphe, basal ganglia, thalamus and the amygdala at PET 3 (see Fig. 2c). Indeed, this might be explained by a more pronounced SERT internalization after prolonged intake of antidepressants (Benmansour et al., 1999). Additionally, since SERT expression and activity seems to be usage-dependent (Ramamoorthy and Blakely, 1999; Steiner et al., 2008), one can expect increased SERT down-regulation in brain regions exhibiting higher SERT density, given the increased occupancy in these regions, which is in accordance with our findings. Although increased SERT down-regulation might be expected in brainstem and other subcortical regions with high SERT density, this does not contradict theoretical concepts which link clinical response to SERT down-regulation primarily in projection areas (Best et al., 2011). Indeed, a recent study on the effects of 8–10 weeks of citalopram treatment in geriatric depression found positive correlations between SERT occupancy and treatment response only in cortical and limbic regions (Smith et al., 2011). Still, as drug plasma levels were significantly elevated after prolonged treatment (see Sample characteristics section), our results may be also explained by increased drug concentrations in regions with high target density.

The third aim of the present study was to investigate the association between regional SERT occupancies and escitalopram plasma levels (Q4). Although we did not detect a significant correlation between SERT occupancy and escitalopram plasma levels 6 h after the first drug intake (PET 2), strong correlations were observed after approximately three weeks of SSRI administration in subcortical regions including the DRN, thalamus, caudate and putamen. The lack of correlation for the second PET measurement may be explained by influence of the active metabolite desmethylcitalopram which was not analyzed in the present study. Furthermore, short time-intervals, e.g., between blood sampling and during PET scan 6 h after single drug dose (PET 2) might cause relevant differences in plasma level concentrations. A second measurement of plasma drug concentrations after the PET scan might have revealed variations during the measurements, which was not done in the present study. Still, several PET studies have established the association between SERT occupancy after chronic intake of different antidepressant agents (amitryptiline, clomipramine, fluoxetine, citalopram, venlafaxine, sertraline, paroxetine) and plasma levels (Lundberg et al., 2012; Meyer et al., 2004). These findings imply that the region-specific impact of antidepressant agents on SERT occupancy only becomes evident after chronic SSRI intake. As SSRIs' antidepressant effect is known to commence after a latency period of several weeks (Blier and de Montigny, 1999; El Mansari et al., 2005), one may link plasma concentrations of the drug to treatment efficacy only after its effect on SERT occupancy has been established.

It is worth mentioning that our results are mostly in agreement, regardless of a ROI-based or a voxel-wise approach. However, some inconsistencies between both approaches remain, which may be attributed to inhomogeneity in SERT occupancy and thus SERT density even within a defined brain region. This is in accordance with previous findings using postmortem quantitative receptor autoradiography, showing that the distribution of serotonin receptors do not necessarily follow the common parcellations based on the cytoarchitecture defined in neuroanatomical atlases such as Brodmann's or AAL (Scheperjans et al., 2005; Zilles and Amunts, 2009).

Several issues should be considered in the interpretation of the results of the present investigation. A limitation within this study is that arterial blood sampling was not performed. Therefore, we are not able to estimate specific binding within the reference region (Hinz

et al., 2008; Parsey et al., 2006), as the cerebellar gray matter was shown to exhibit quantifiable and displaceable SERT (Parsey et al., 2006). Thus, estimations of SERT BP_{ND} may have been underestimated. As we found occupancy to be positively correlated with pretreatment SERT BP_{ND}, lower occupancy in the cerebellar gray matter compared to regions with high BP_{ND} may be expected. Therefore, underestimations of residual SERT BP_{ND} should be more pronounced in regions with high SERT BP_{ND} after acute and chronic drug intake, therefore leading to an overestimation of occupancies in these regions. Still, previous studies based on post-mortem autoradiography identified the cerebellar gray matter excluding vermis as optimal reference region for [^{11}C]DASB occupancy studies (Parsey et al., 2006). Finally, the treatment period of our study sample was 24.73 ± 3.3 days (for details see Lanzenberger et al., 2012), which is relatively short in the context of SERT occupancy studies, which typically apply four weeks as the minimum duration for the intake of antidepressants (Meyer et al., 2001, 2004; Smith et al., 2011). However, recent simulation studies suggest SERT down-regulation to underlie the mechanisms associated with treatment response (Best et al., 2011) and animal research suggests a marked down-regulation of SERT already after 15 to 21 days of continuous administration of sertraline (Benmansour et al., 2002).

Conclusion

The results of this study indicate regional differences in serotonin transporter occupancy by acute and prolonged treatment with SSRIs. Furthermore, our study reveals a strong but regionally restricted dependence of SERT blockage on pretreatment transporter availability as well as drug plasma concentrations. These findings may substantiate the postulated link between treatment response and SSRI blockage of the SERT while confining it to certain brain regions such as the subgenual cingulate cortex.

Role of funding source

Personal costs were partly funded by the Medical University of Vienna and Austrian national research funding agencies (FWF, OeNB) to R. Lanzenberger, PET measurements and treatment were supported by an investigator-initiated and unrestricted research grant from H. Lundbeck A/S, Denmark to S. Kasper. H. Lundbeck A/S, FWF and OeNB had no further role in study design; in the collection, analysis and interpretation of data; in the writing of the report and in the decision to submit the paper for publication.

Contributors

R. Lanzenberger and S. Kasper designed the main study. G.S. Kranz, P. Baldinger, M. Spies and A. Höflich established the details of analysis and study concept, M. Savli, G.S. Kranz and A. Hahn performed the data analyses. W. Wadsak, M. Mitterhauser, D. Haeusler and C. Philippe performed the radiotracer synthesis and supported the PET procedures. P. Baldinger and G.S. Kranz wrote the first draft of the manuscript. All authors contributed to and have approved the final manuscript.

Acknowledgments

The authors are grateful to U. Moser, E. Akimova, C. Spindelegger, M. Fink, M. Willeit, G. Karanikas, K. Kletter and the clinical staff at the PET center for their medical support, and H. Sitte for advisory service. We are especially indebted to G. Wagner, B. Reiterits, I. Leitinger, and R. Bartosch for technical support during the PET scans.

Conflict of interest

S. Kasper declares that he has received grant/research support from Bristol Myers-Squibb, Eli Lilly, GlaxoSmithKline, Lundbeck, Organon, Sepracor and Servier; has served as a consultant or on advisory boards for AstraZeneca, Bristol-Myers Squibb, Eli Lilly, GlaxoSmithKline, Janssen, Lundbeck, Merck Sharp and Dome (MSD), Novartis, Organon, Pfizer, Schwabe, Sepracor, and Servier; and has served on speakers' bureaus for Angelini, AstraZeneca, Bristol Myers-Squibb, Eli Lilly, Janssen, Lundbeck, Pfizer, Pierre Fabre, Schwabe, Sepracor, and Servier. R. Lanzenberger received travel grants and conference speaker honoraria from AstraZeneca, Roche and Lundbeck A/S. M. Mitterhauser and W. Wadsak received speaker honoraria from Bayer. P. Baldinger, M Spies, and G.S. Kranz received travel grants from Roche and AOP Orphan Pharmaceuticals. A. Hahn was recipient of a DOC-fellowship of the Austrian Academy of Sciences at the Department of Psychiatry and Psychotherapy. The authors D. Haeusler, C. Philippe, A. Höflich, and M. Savli report no financial relationships with commercial interests.

Appendix A. Supplementary data

Supplementary data to this article can be found online at http://dx.doi.org/10.1016/j.neuroimage.2013.10.002.

References

Benmansour, S., Cecchi, M., Morilak, D.A., Gerhardt, G.A., Javors, M.A., Gould, G.G., Frazer, A., 1999. Effects of chronic antidepressant treatments on serotonin transporter function, density, and mRNA level. J. Neurosci. 19, 10494–10501.

Benmansour, S., Owens, W.A., Cecchi, M., Morilak, D.A., Frazer, A., 2002. Serotonin clearance in vivo is altered to a greater extent by antidepressant-induced downregulation of the serotonin transporter than by acute blockade of this transporter. J. Neurosci. 22, 6766–6772.

Best, J., Nijhout, H.F., Reed, M., 2011. Bursts and the efficacy of selective serotonin reuptake inhibitors. Pharmacopsychiatry 44 (Suppl. 1), S76–S83.

Blier, P., de Montigny, C., 1999. Serotonin and drug-induced therapeutic responses in major depression, obsessive-compulsive and panic disorders. Neuropsychopharmacology 21, 91S–98S.

El Mansari, M., Sanchez, C., Chouvet, G., Renaud, B., Haddjeri, N., 2005. Effects of acute and long-term administration of escitalopram and citalopram on serotonin neurotransmission: an in vivo electrophysiological study in rat brain. Neuropsychopharmacology 30, 1269–1277.

Fink, M., Wadsak, W., Savli, M., Stein, P., Moser, U., Hahn, A., Mien, L.-K., Kletter, K., Mitterhauser, M., Kasper, S., Lanzenberger, R., 2009. Lateralization of the serotonin-1A receptor distribution in language areas revealed by PET. NeuroImage 45, 598–605.

Garris, P.A., Wightman, R.M., 1994. Different kinetics govern dopaminergic transmission in the amygdala, prefrontal cortex, and striatum: an in vivo voltammetric study. J. Neurosci. 14, 442–450.

Gill, J.S., Beevers, D.G., Zezulka, A.V., Davies, P., 1985. Relation between initial blood pressure and its fall with treatment. Lancet 325, 567–569.

Grunder, G., Landvogt, C., Vernaleken, I., Buchholz, H.G., Ondracek, J., Siessmeier, T., Hartter, S., Schreckenberger, M., Stoeter, P., Hiemke, C., Rosch, F., Wong, D.F., Bartenstein, P., 2006. The striatal and extrastriatal D2/D3 receptor-binding profile of clozapine in patients with schizophrenia. Neuropsychopharmacology 31, 1027–1035.

Grunder, G., Fellows, C., Janouschek, H., Veselinovic, T., Boy, C., Brocheler, A., Kirschbaum, K.M., Hellmann, S., Spreckelmeyer, K.M., Hiemke, C., Rosch, F., Schaefer, W.M., Vernaleken, I., 2008. Brain and plasma pharmacokinetics of aripiprazole in patients with schizophrenia: an [18F]fallypride PET study. Am. J. Psychiatry 165, 988–995.

Haeusler, D., Mien, L.K., Nics, L., Ungersboeck, J., Philippe, C., Lanzenberger, R.R., Kletter, K., Dudczak, R., Mitterhauser, M., Wadsak, W., 2009. Simple and rapid preparation of [11C]DASB with high quality and reliability for routine applications. Appl. Radiat. Isot. 67, 1654–1660.

Hinz, R., Selvaraj, S., Murthy, N.V., Bhagwagar, Z., Taylor, M., Cowen, P.J., Grasby, P.M., 2008. Effects of citalopram infusion on the serotonin transporter binding of [11C] DASB in healthy controls. J. Cereb. Blood Flow Metab. 28, 1478–1490.

Hoflich, A., Baldinger, P., Savli, M., Lanzenberger, R., Kasper, S., 2012. Imaging treatment effects in depression. Rev. Neurosci. 23, 227–252.

Ichise, M., Liow, J.S., Lu, J.Q., Takano, A., Model, K., Toyama, H., Suhara, T., Suzuki, K., Innis, R.B., Carson, R.E., 2003. Linearized reference tissue parametric imaging methods: application to [11C]DASB positron emission tomography studies of the serotonin transporter in human brain. J. Cereb. Blood Flow Metab. 23, 1096–1112.

Innis, R.B., Cunningham, V.J., Delforge, J., Fujita, M., Gjedde, A., Gunn, R.N., Holden, J., Houle, S., Huang, S.-C., Ichise, M., Iida, H., Ito, H., Kimura, Y., Koeppe, R.A., Knudsen, G.M., Knuuti, J., Lammertsma, A.A., Laruelle, M., Logan, J., Maguire, R.P., Mintun, M.A., Morris, E.D., Parsey, R., Price, J.C., Slifstein, M., Sossi, V., Suhara, T., Votaw, J.R., Wong, D.F., Carson, R.E., 2007. Consensus nomenclature for in vivo imaging of reversibly binding radioligands. J. Cereb. Blood Flow Metab. 27, 1533–1539.

Kasper, S., Sacher, J., Klein, N., Mossaheb, N., Attarbaschi-Steiner, T., Lanzenberger, R., Spindelegger, C., Asenbaum, S., Holik, A., Dudczak, R., 2009. Differences in the dynamics of serotonin reuptake transporter occupancy may explain superior clinical efficacy of escitalopram versus citalopram. Int. Clin. Psychopharmacol. 24, 119–125.

Kegeles, L.S., Slifstein, M., Frankle, W.G., Xu, X., Hackett, E., Bae, S.A., Gonzales, R., Kim, J.H., Alvarez, B., Gil, R., Laruelle, M., Abi-Dargham, A., 2008. Dose-occupancy study of

striatal and extrastriatal dopamine D2 receptors by aripiprazole in schizophrenia with PET and [18F]fallypride. Neuropsychopharmacology 33, 3111–3125.
Kingback, M., Carlsson, B., Ahlner, J., Bengtsson, F., Kugelberg, F.C., 2011. Cytochrome P450-dependent disposition of the enantiomers of citalopram and its metabolites: in vivo studies in Sprague–Dawley and Dark Agouti rats. Chirality 23, 172–177.
Kranz, G.S., Kasper, S., Lanzenberger, R., 2010. Reward and the serotonergic system. Neuroscience 166, 1023–1035.
Kranz, G.S., Hahn, A., Savli, M., Lanzenberger, R., 2012. Challenges in the differentiation of midbrain raphe nuclei in neuroimaging research. Proc. Natl. Acad. Sci. 109, E2000.
Kugelberg, F.C., Apelqvist, G., Carlsson, B., Ahlner, J., Bengtsson, F., 2001. In vivo steady-state pharmacokinetic outcome following clinical and toxic doses of racemic citalopram to rats. Br. J. Pharmacol. 132, 1683–1690.
Kugelberg, F.C., Carlsson, B., Ahlner, J., Bengtsson, F., 2003. Stereoselective single-dose kinetics of citalopram and its metabolites in rats. Chirality 15, 622–629.
Kugelberg, F.C., Druid, H., Carlsson, B., Ahlner, J., Bengtsson, F., 2004. Postmortem redistribution of the enantiomers of citalopram and its metabolites: an experimental study in rats. J. Anal. Toxicol. 28, 631–637.
Lanzenberger, R., Kranz, G.S., Haeusler, D., Akimova, E., Savli, M., Hahn, A., Mitterhauser, M., Spindelegger, C., Philippe, C., Fink, M., Wadsak, W., Karanikas, G., Kasper, S., 2012. Prediction of SSRI treatment response in major depression based on serotonin transporter interplay between median raphe nucleus and projection areas. Neuroimage 63, 874–881.
Laruelle, M., Slifstein, M., Huang, Y., 2003. Relationships between radiotracer properties and image quality in molecular imaging of the brain with positron emission tomography. Mol. Imaging Biol. 5, 363–375.
Lawler, C.P., Prioleau, C., Lewis, M.M., Mak, C., Jiang, D., Schetz, J.A., Gonzalez, A.M., Sibley, D.R., Mailman, R.B., 1999. Interactions of the novel antipsychotic aripiprazole (OPC-14597) with dopamine and serotonin receptor subtypes. Neuropsychopharmacology 20, 612–627.
Lundberg, J., Tiger, M., Landén, M., Halldin, C., Farde, L., 2012. Serotonin transporter occupancy with TCAs and SSRIs: a PET study in patients with major depressive disorder. Int. J. Neuropsychopharmacol. 15, 1167–1172.
Mayberg, H.S., 2009. Targeted electrode-based modulation of neural circuits for depression. J. Clin. Invest. 119, 717–725.
Meyer, J.H., 2007. Imaging the serotonin transporter during major depressive disorder and antidepressant treatment. J. Psychiatry Neurosci. 32, 86–102.
Meyer, J.H., Wilson, A.A., Ginovart, N., Goulding, V., Hussey, D., Hood, K., Houle, S., 2001. Occupancy of serotonin transporters by paroxetine and citalopram during treatment of depression: a [(11)C]DASB PET imaging study. Am. J. Psychiatry 158, 1843–1849.
Meyer, J.H., Wilson, A.A., Sagrati, S., Hussey, D., Carella, A., Potter, W.Z., Ginovart, N., Spencer, E.P., Cheok, A., Houle, S., 2004. Serotonin transporter occupancy of five selective serotonin reuptake inhibitors at different doses: an [11C]DASB positron emission tomography study. Am. J. Psychiatry 161, 826–835.
Oldham, P.D., 1962. A note on the analysis of repeated measurements of the same subjects. J. Chron. Dis. 15, 969–977.
Parsey, R.V., Kent, J.M., Oquendo, M.A., Richards, M.C., Pratap, M., Cooper, T.B., Arango, V., Mann, J.J., 2006. Acute occupancy of brain serotonin transporter by sertraline as measured by [11C]DASB and positron emission tomography. Biol. Psychiatry 59, 821–828.
Pilowsky, L.S., Mulligan, R.S., Acton, P.D., Ell, P.J., Costa, D.C., Kerwin, R.W., 1997. Limbic selectivity of clozapine. Lancet 350, 490–491.
Ramamoorthy, S., Blakely, R.D., 1999. Phosphorylation and sequestration of serotonin transporters differentially modulated by psychostimulants. Science 285, 763–766.
Savli, M., Bauer, A., Mitterhauser, M., Ding, Y.-S., Hahn, A., Kroll, T., Neumeister, A., Haeusler, D., Ungersboeck, J., Henry, S., Isfahani, S.A., Rattay, F., Wadsak, W., Kasper, S., Lanzenberger, R., 2012. Normative database of the serotonergic system in healthy subjects using multi-tracer PET. NeuroImage 63, 447–459.
Scheperjans, F., Grefkes, C., Palomero-Gallagher, N., Schleicher, A., Zilles, K., 2005. Subdivisions of human parietal area 5 revealed by quantitative receptor autoradiography: a parietal region between motor, somatosensory, and cingulate cortical areas. Neuroimage 25, 975–992.
Seeman, P., 2002. Atypical antipsychotics: mechanism of action. Can. J. Psychiatry 47, 27–38.
Smith, G.S., Kahn, A., Sacher, J., Rusjan, P., van Eimeren, T., Flint, A., Wilson, A.A., 2011. Serotonin transporter occupancy and the functional neuroanatomic effects of citalopram in geriatric depression. Am. J. Geriatr. Psychiatry 19, 1016–1025.
Stein, P., Savli, M., Wadsak, W., Mitterhauser, M., Fink, M., Spindelegger, C., Mien, L.-K., Moser, U., Dudczak, R., Kletter, K., Kasper, S., Lanzenberger, R., 2008. The serotonin-1A receptor distribution in healthy men and women measured by PET and [carbonyl-11C]WAY-100635. Eur. J. Nucl. Med. Mol. Imaging 35, 2159–2168.
Steiner, J.A., Carneiro, A.M., Blakely, R.D., 2008. Going with the flow: trafficking-dependent and -independent regulation of serotonin transport. Traffic 9, 1393–1402.
Takahata, K., Ito, H., Takano, H., Arakawa, R., Fujiwara, H., Kimura, Y., Kodaka, F., Sasaki, T., Nogami, T., Suzuki, M., Nagashima, T., Shimada, H., Kato, M., Mimura, M., Suhara, T., 2012. Striatal and extrastriatal dopamine D(2) receptor occupancy by the partial agonist antipsychotic drug aripiprazole in the human brain: a positron emission tomography study with [^{11}C]raclopride and [^{11}C]FLB457. Psychopharmacology (Berl) 222, 165–172.
Talbot, P.S., Laruelle, M., 2002. The role of in vivo molecular imaging with PET and SPECT in the elucidation of psychiatric drug action and new drug development. Eur. Neuropsychopharmacol. 12, 503–511.
Tu, Y.K., Gilthorpe, M.S., 2007. Revisiting the relation between change and initial value: a review and evaluation. Stat. Med. 26, 443–457.
Tzourio-Mazoyer, N., Landeau, B., Papathanassiou, D., Crivello, F., Etard, O., Delcroix, N., Mazoyer, B., Joliot, M., 2002. Automated anatomical labeling of activations in SPM using a macroscopic anatomical parcellation of the MNI MRI single-subject brain. NeuroImage 15, 273–289.
Urban, J.D., Clarke, W.P., von Zastrow, M., Nichols, D.E., Kobilka, B., Weinstein, H., Javitch, J.A., Roth, B.L., Christopoulos, A., Sexton, P.M., Miller, K.J., Spedding, M., Mailman, R.B., 2007. Functional selectivity and classical concepts of quantitative pharmacology. J. Pharmacol. Exp. Ther. 320, 1–13.
Vauquelin, G., Charlton, S.J., 2010. Long-lasting target binding and rebinding as mechanisms to prolong in vivo drug action. Br. J. Pharmacol. 161, 488–508.
Vernaleken, I., Fellows, C., Janouschek, H., Brocheler, A., Veselinovic, T., Landvogt, C., Boy, C., Buchholz, H.G., Spreckelmeyer, K., Bartenstein, P., Cumming, P., Hiemke, C., Rosch, F., Schafer, W., Wong, D.F., Grunder, G., 2008. Striatal and extrastriatal D2/D3-receptor-binding properties of ziprasidone: a positron emission tomography study with [18F]fallypride and [11C]raclopride (D2/D3-receptor occupancy of ziprasidone). J. Clin. Psychopharmacol. 28, 608–617.
Xiberas, X., Martinot, J.L., Mallet, L., Artiges, E., Canal, M., Loc'h, C., Maziere, B., Paillere-Martinot, M.L., 2001. In vivo extrastriatal and striatal D2 dopamine receptor blockade by amisulpride in schizophrenia. J. Clin. Psychopharmacol. 21, 207–214.
Zeng, Z., Chen, T.-B., Miller, P.J., Dean, D., Tang, Y.S., Sur, C., Williams Jr., D.L., 2006. The serotonin transporter in rhesus monkey brain: comparison of DASB and citalopram binding sites. Nucl. Med. Biol. 33, 555–563.
Zilles, K., Amunts, K., 2009. Receptor mapping: architecture of the human cerebral cortex. Curr. Opin. Neurol. 22, 331–339.